IEEE Access
Multidisciplinary ⋮ Rapid Review ⋮ Open Access Journal

Received 16 May 2023, accepted 4 June 2023, date of publication 22 June 2023, date of current version 13 July 2023.

Digital Object Identifier 10.1109/ACCESS.2023.3288486

RESEARCH ARTICLE

A Medium to Long-Term Multi-Influencing Factor Copper Price Prediction Method Based on CNN-LSTM

FEI LI[1], **HANLU ZHOU**[2], **MIN LIU**[2], **AND LEIMING DING**[1,3]

[1]School of Computer and Computing Science, Hangzhou City University, Hangzhou, Zhejiang 310015, China
[2]School of Electronics and Information Engineering, Tongji University, Shanghai 201804, China
[3]School of Computer Science and Technology, Zhejiang University of Technology, Hangzhou 310015, China

Corresponding author: Fei Li (lif@hzcu.edu.cn)

This work was supported in part by the National Natural Science Foundation of China under Project 62273261, in part by the Hangzhou Key Laboratory for Internet of Things (IoT) Technology and Application, in part by the SuperComputing Center of Hangzhou City University, and in part by the Zhejiang Engineering Laboratory Intelligent Plant Factory.

ABSTRACT Non-ferrous copper prices exhibit high noise, non-smoothness, and non-linearity, which pose significant challenges to accurate price prediction. One of the current methods for predicting copper prices is multi-influencing factor analysis, which typically relies on traditional optimization or neural network methods to identify factors that affect copper prices. However, extracting attribute features and high-level semantics from raw data using these conventional methods can be difficult, which may necessitate revision of the selected influencing factors and final results. This paper proposes a CNN-LSTM-based approach that leverages the feature extraction capabilities of Convolutional Neural Networks (CNN) and Long Short-Term Memory (LSTM) networks. After analyzing the fluctuation features of copper prices and their qualitative relationships with factors such as supply and demand, energy costs, alternative metals, global macroeconomic conditions, and national policies, we selected 11 influencing factors for copper price fluctuation as explanatory variables using scatter plots, Pearson correlation coefficients, and heat maps. These variables are then fed into a CNN-LSTM network as a two-dimensional multivariate time series, along with historical copper price data, for monthly price forecasting. Experimental results show that our proposed method outperforms other existing methods by utilizing the attribute space feature extraction capability of CNNs and the temporal feature extraction of LSTMs.

INDEX TERMS Convolutional neural network, long short-term memory, multi-influencing factor, correlation analysis, price prediction.

I. INTRODUCTION

Non -ferrous metals are crucial raw materials and strategic resources for national economic development and defense technology. They find wide applications in power electronics, household appliances, transportation energy, machinery manufacturing, and construction [1], [2], [3]. In electronic applications, for example, copper can be used to make circuit boards, wires and cables for its good electrical conductivity, and it can be also used to make heat sinks for electronic devices because of its thermal conductivity. In addition, copper can be used for RF protection, connectors, and more. The prices of non-ferrous metals have a significant impact on the development of production, supply, and marketing integration plans. By forecasting the prices of non-ferrous metals, enterprises can better understand future market fluctuations, assist decision-makers in developing early risk strategies, and establish reasonable integration plans to enhance their business performance. Thus, research and application of future price prediction methods hold far-reaching practical significance.

Non-ferrous metals have both commodity and financial attributes, and their price fluctuations are influenced by numerous factors. As commodities, global supply and

The associate editor coordinating the review of this manuscript and approving it for publication was Sajid Ali.

demand, as well as energy costs for smelting and production, shape the medium and long-term trend of non-ferrous metal prices. On the other hand, the financial attributes of non-ferrous metals, such as the U.S. dollar exchange rate, consumer indices, and price levels, contribute to their short-term volatility [4]. Moreover, the various influencing factors are often coupled and interrelated with each other, resulting in the historical price series of non-ferrous metals exhibiting high volatility and a complex fluctuation pattern. Specifically, this pattern is characterized by apparent high noise, non-smoothness, and non-linearity, making accurate prediction of non-ferrous metal prices a complicated and challenging scientific problem [5].

At present, the primary method for forecasting non-ferrous metal prices is to analyze the various factors influencing their price fluctuations, such as supply and demand, inventory levels, production costs, economic indicators, national policies, and unexpected events. Based on the historical price series of non-ferrous metals and the past data of relevant influencing factors, reasonable judgments and predictions on future prices are made using statistical and mathematical methods. In recent years, with the rapid advancement of machine learning, deep learning, and other technologies, non-ferrous metal price prediction methods with multi-influencing factors have emerged. With sufficient historical data, these advanced methods have proven to be capable of making more accurate predictions on future prices.

However, due to the non-linear relationship between each factor and historical price data, there is still considerable room for improving the accuracy of multi-factor forecasting methods. Traditional neural networks and optimization algorithms alone are incapable of extracting high-level semantic features, requiring further refinement of the approach.

Therefore, this paper proposed a CNN-LSTM-based non-ferrous metal price prediction algorithm. Specifically, the contributions of this study are:

1) We examined the volatility characteristics of copper prices, a non-ferrous metal, and investigated the evolution of the global copper market in light of various uncertainties, including supply and demand fluctuations, energy costs, competition from alternative metals, overall macroeconomic conditions, and national policies.
2) Using correlation analysis techniques, we identified the 11 most significant factors that influence copper prices. These include refined copper production, refined copper stocks, refined copper consumption, natural gas, gold, silver, zinc, the U.S. dollar index, coffee, soybeans, and lean pigs, which serve as explanatory variables for fluctuations in copper prices.
3) We propose a CNN-LSTM-based price prediction method for two-dimensional multivariate time series, which is different from previous applications on one-dimensional time series, and we demonstrated its effectiveness and accuracy through experimentation.

The rest of the paper is organized as follows: Section II reviews the primary methods for predicting non-ferrous metals or copper prices. Section III introduces the theory of CNN and LSTM. Section IV describes the volatility characteristics of copper prices and lists the possible influencing factors. Section V uses scatter plots, Pearson correlation coefficient and heat map method to optimize and get top 11 influencing factors. Section VI introduces CNN-LSTM networks and copper price prediction methods. Section VII gives the experimental validation, and Section VIII discusses the conclusions and future work.

II. RELATED WORKS

Over the past few decades, non-ferrous metal price prediction has garnered significant attention and been extensively investigated by scholars. There are two primary methods for forecasting price series data: the raw data price prediction method and the multi-influencing factor price prediction method, which differ in their input signals.

A. RAW DATA PRICE PREDICTION METHOD

This method takes historical price series data as input and employs mathematical techniques, such as mathematical regression and neural networks, to forecast future prices.

Previous research mainly relied on statistical techniques such as Autoregressive Moving Average (ARMA) [8], Differential Autoregressive Moving Average (ARIMA, Autoregressive Integrated Moving Average) [9], [10], Auto-Regressive Conditional Heteroskedasticity (ARCH) [11], Generalized Auto Regressive Conditional Heteroskedasticity (GARCH) [12], and Conditional Heteroskedasticity (ARCH) [13] to implement the raw data price prediction method.

Other advanced statistical methods have been developed for non-ferrous metal price prediction as well. García and Kristjanpolller [13] combined a fuzzy inference system (FIS) with the GARCH model to create an adaptive prediction model for forecasting monthly copper price changes. Hadavandi et al. [14] introduced a Particle Swarm Optimization algorithm (PSO) time series prediction model, while Zhao et al. [15] proposed a generalized pattern-matching model based on a genetic algorithm (GPEGA) that incorporates empirical distribution. Alameer et al. [16] presented an improved adaptive neuro-fuzzy inference system (ANFIS).

Statistical models for forecasting assume that the original data undergo linear transformations. However, there is no evidence to suggest that price data are intrinsically linear, limiting the effectiveness of statistical models for long-term predictions. As iterations accumulate during the forecasting process, prediction errors can have a negative impact on the final accuracy of these models.

When faced with frequent and drastic fluctuations in prices, some approaches have incorporated artificial intelligence (AI) algorithms to address the non-linear nature of non-ferrous metal price changes. For instance, Dehghani and Bogdanovic [17] used the Brownian motion mean reversion model (BMMR) to forecast copper prices. Lasheras et al. [18] analyzed copper spot price data from the New York Mercantile Exchange using three models-ARIMA, Multi-Layer Perceptron (MLP), and local regression network Elman- respectively, to conduct forecasting experiments.

A comparative analysis of statistical methods, artificial intelligence algorithms, and machine learning techniques reveals that machine learning and neural network methods are superior to statistical models in identifying non-linear features in price series and delivering more accurate predictions. Nevertheless, the inherent non-linearity and non-smoothness of one-dimensional price series data, combined with the complex and subtle fluctuation patterns unique to non-ferrous metals, make it difficult for simple forecasting models to extract deep-level feature information from one-dimensional price data alone. This renders future price forecasting for non-ferrous metals a challenging task.

B. MULTI-INFLUENCING PRICE PREDICTION METHOD

The multi-influencing factor price forecasting method involves analyzing numerous intricate factors that impact price fluctuations, and incorporating them into the prediction model as explanatory variables to make reasonable and precise forecasts of future prices. Generally speaking, the quality of the influencing factors predominantly affects the final prediction outcomes, with better-quality influencing factors resulting in higher accuracy of predictions.

Traditional forecasting methods relying on multiple influencing factors, typically involve qualitative analysis, as demonstrated by Ciner and other researchers [19], who experimentally established a strong correlation between exchange rate fluctuations of the South African currency and price fluctuations of palladium and platinum. In another study, Frankel et al. [20] analyzed relevant factors impacting non-ferrous metal prices in the London Metal Exchange, such as inflation/deflation levels and appropriate fiscal policies, while also taking into account macroeconomic and micro-market currency and exchange rate factors. Behmiri and Manera [21] investigated the impact of oil price shocks on the price volatility of various metals, including aluminium, copper, lead, nickel, tin, zinc, gold, silver, palladium, and platinum, and found that oil price shocks affect each metal's price volatility to varying degrees. Mo et al. [22] explored the dynamic relationship between the U.S. dollar, crude oil, and gold markets, concluding that the dynamic correlation between gold and oil is always positive.

Furthermore, there are significant correlations between different types of non-ferrous metals. Ozdemir et al. [23] used LSTM and GRU forecasting models based on historical monthly price data of non-ferrous metals from March 1991 to May 2021 to conduct experiments. Their findings showed that prices of metals such as aluminium, copper, gold, silver, zinc, iron and lead have an impact on the future fluctuations of nickel prices to some extent. Additionally, Buncic [24] discovered a strong correlation between copper prices and the costs of gold and silver, due to copper becoming a substitute for precious metals like gold and silver in the investment field.

In recent years, the availability of massive data and advanced data mining techniques has led more researchers to focus on multi-influencing factor forecasting, resulting in a flourishing of data-driven multi-influencing factor price prediction methods. These big data-driven forecasting techniques have been found to exhibit higher prediction accuracy and robustness when compared to traditional qualitative analysis-based predictions. One major advantage is the ability to automatically extract feature information from the input data, thus producing a more accurate representation of the input data.

Feature extraction-based machine learning algorithms have become a widely used approach for non-ferrous metal price forecasting. For instance, Aye et al. [25] categorized gold price influencing factors into six categories and utilized the principal component analysis (PCA) method to predict prices with 28 unclassified factors. Similarly, Liu et al. [26] conducted a correlation analysis by the Pearson correlation coefficient method between copper prices and eight influencing factors including the Dow Jones index, crude oil, and gold, and established a decision tree for copper price forecasting based on the multi-dimensional data model. This approach demonstrated high accuracy and robustness in multi-influencing factor prediction. Building upon Liu's work, Díaz et al. [27] further proposed an improved copper price forecasting method, which utilized random forest and gradient-enhanced regression trees for short- and long-term forecasting of future copper prices. The experimental results showed that random forest and gradient-enhanced regression tree models outperformed regression tree models.

Deep learning algorithms have been increasingly applied in multi-influencing factor price analysis due to their powerful feature learning capability. For example, Zhang et al. [28] considered variables such as US CPI, federal funds rate, crude oil futures price, nominal effective exchange rate, and Dow Jones index as highly correlated with the gold price, and proposed a deep belief network (DBN)-based multi-influencing factor price forecasting method using monthly gold price data published in the London market as output. Similarly, Alameer et al. [29] studied the correlation between various economic factors and gold price, copper price, iron ore price, silver price, oil price, Chinese exchange rate, Indian exchange rate, South African exchange rate, Chinese inflation rate, and U.S. inflation rate, and utilized the latest meta-heuristic Whale Optimization Algorithm (WOA) as a trainer to learn multi-layer perceptron neural networks. Their improved deep learning model WOA-NN accurately predicted long-term monthly fluctuations in gold prices, outperforming basic models such as ARIMA. Zhang et al. [30] focused on crude oil, natural gas, gold, silver, and iron ore parameters as influencing factors of copper price, and also considered the exchange rates of the four largest copper-producing countries, Chile, China, Peru, and Australia. They predicted future monthly copper prices using an extreme learning machine prediction model optimized by the PSO and genetic algorithms. The experimental results confirmed the correlation between the above factors and copper price fluctuations.

Based on the above analysis, the multi-influencing factor price forecasting method involves inputting complex factors that affect the medium and long-term trend and short-term fluctuations of metal prices into the forecasting model as explanatory variables for price fluctuations. Since multiple influencing factors exist in the same market and interact with each other, their interrelationships may not be apparent in the short term, making this method more suitable for price forecasting over longer periods.

The accuracy of multi-influencing factor prediction methods is heavily dependent on the quality of the selected factors. The selection of relevant factors requires economic expertise and extensive investigation, and cannot be determined through qualitative analysis alone. Even with the help of optimization algorithms and traditional neural networks, it remains challenging to confirm the relationships between influencing factors. Therefore, new methods need to be explored to quantitatively calculate the correlation coefficients between selected factors and prices and to determine the influencing factors in a more rational manner.

III. THEORETICAL BACKGROUND

A. CNN

The convolutional neural network is a typical deep learning model, and the main structure contains three parts: convolutional layer, pooling layer and fully connected layer [31], which extracts features from the input multi-dimensional data through convolutional and pooling layers and then performs feature fusion through the fully connected layer.

With the convolutional layer, the CNN can capture local features from the input data. By stacking these local features, it obtains global features that are further downscaled using the pooling layer. The operation is defined as

$$x_i^j = f(\sum k = 1^n W_{i,k}^j * x_k^{j-1} + b_i^j) \tag{1}$$

where x_i^j donates the ith output feature map of jth level; x_k^{j-1} donates the kth input feature map of $(j-1)$th level; $W_{i,k}^j$ is the convolution kernel between the ith output feature map at the jth layer and kth input feature map at the $(j-1)$th layer; n is the number of the input feature maps; b_i^j is the bias of the ith output feature map at the jth layer; $f(x)$ is the activation function. In this paper, ReLU is used as follows due to its excellent performance:

$$x_i^j = \max(0, x_i^j) \tag{2}$$

B. LSTM

Traditional neural networks are not well-suited for accurately extracting feature information from time-series data along the time dimension, making them ill-equipped to handle historical copper prices and related influencing factors. However, Recurrent Neural Networks (RNNs) have emerged as a solution to such problems. RNNs are composed of multiple identical non-linear nodes that are internally connected in a recursive chain. This configuration enables information to be recursively transmitted along the direction of input data advancement, imbuing RNNs with a memory function that ensures practical information can persistently flow through the network.

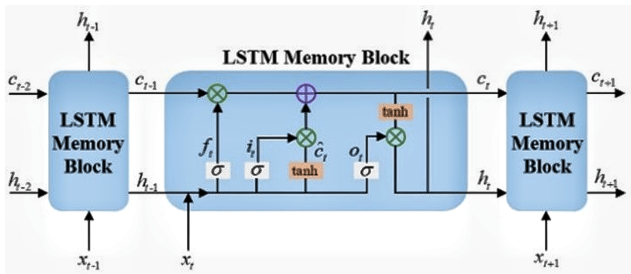

FIGURE 1. LSTM network structure.

LSTM addresses the long-term dependency problem inherent in RNNs [32]. Unlike RNNs, LSTM introduces more complex gating signals in its structure to control information flow. The memory unit of LSTM is composed of three parts: the forgetting gate, input gate, and output gate. Fig. 1 illustrates the network architecture.

As shown in Fig. 1, the LSTM cell state is internally composed of four feedforward networks, including one Tanh activation function and three σ functions. x_t denotes the input of the current cell state, h_t denotes the output information, c_t denotes the memory cell state output, and f_t, i_t and o_t denote the forgetting gate, input gate and output gate, respectively, where the forgetting gate is specifically used to store the past state information, which can be very effective in processing and retaining the long-term memory. At a particular moment, the input information in the cell includes the sample features of the current moment and passes the historical state over, and outputs the current cell state after being processed by several activation functions. The key idea that LSTM can achieve long-term memory lies in its cell state. By these three gating signals, the LSTM can control the historical and the current input and determine to what extent the current output is.

The LSTM network update process can be divided into three steps:

1) The forget gate determines the information to be forgotten, which can be expressed using Eq. (3):

$$f_t = \sigma(W_f * [h_{t-1}, x_t] + b_f) \tag{3}$$

In Eq. (3), W_f and b_f represent the weight matrix and bias term of the forget gate.The multiplication of f_t and c_{t-1} determines which information from the previous cell state is forgotten.

2) The input gate determines the information to be updated, which can be expressed using Eq. (4) - Eq. (6):

$$i_t = \sigma(W_i * [h_{t-1}, x_t] + b_i) \tag{4}$$
$$c_t = \tanh(W_c * [h_{t-1}, x_t] + b_c) \tag{5}$$
$$c_t = f_t * c_{t-1} + i_t * c_t \tag{6}$$

In above equations, W_i, b_i represent the weight matrix and bias term of the input gate, while W_c,b_c represent the weight matrix and bias term of the memory cell state. The input gate signal i_t is multiplied by c_t, deciding which information will be used for updating.

3) The output gate determines the information to be output, which can be expressed using Eq. (7) and Eq. (8):

$$o_t = \sigma(W_o * [h_{t-1}, x_t] + b_o) \tag{7}$$
$$h_t = o_t * \tanh(c_t) \tag{8}$$

In above equations, W_o, b_o represent the weight matrix and bias term of the output gate.

In summary, LSTM is a powerful tool for tackling long-term time-series problems. The historical copper prices and each influencing factor data utilized in this study are time-series data that can be effectively processed by the LSTM network to extract useful time-series features. This approach enables the prediction model to capture long-term trends and relationships, leading to improved prediction accuracy.

C. CNN-LSTM ARCHITECTURE

The price prediction model proposed in this study comprises two interconnected sub-modules, namely the CNN and LSTM networks. The CNN-LSTM network structure is illustrated in Fig. 2.

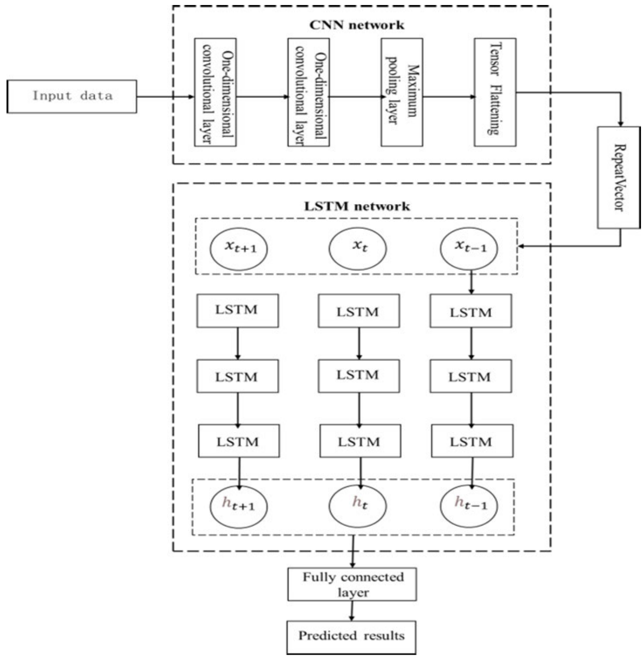

FIGURE 2. CNNL-LSTM network structure.

Two-dimensional time-series data is used as input and another indicator variable (e.g., copper price in this paper) is used as output in CNN-LSTM. Assume that each input data format is (l, w), where l and w denote the length and width of the two-dimensional data respectively, and there are m sample data in total. CNN-LSTM divides the sample data into w channels, each channel is a one-dimensional time-series signal. Each channel data goes through several one-dimensional convolutional layers, a maximum pooling layer, and then the extracted feature vectors are passed through Flatten and RepeatVector operations to obtain some multivariate time series of extracted feature sequences, which are then sent to LTSM for training or prediction.

For one-dimensional time-series signals, LSTM can already achieve better results. Furthermore, the CNN-LSTM structure outperforms the single-model LSTM by exploiting the knowledge extraction of CNN networks and the internal representation learning capability of the temporal data.The main roles of the CNN networks in CNN-LSTM are:

1) Feature extraction: CNNs are very good at automatically learning and extracting useful features from data, without the need for manual feature design and selection. In price forecasting, this may include short-term trends in the market, cyclical patterns.
2) Local perception: CNNs has the ability of local perception due to its convolutional operation, which can identify and extract local patterns in time series, such as sudden price peaks, oscillation patterns of prices.
3) Time Shift Invariance: The CNN has time shift invariance, which means that if a pattern in the time series occurs a displacement, the CNN still recognizes it. This is very useful for processing financial time series, as certain behavior patterns in the market may repeat in different periods.
4) Reducing overfitting: Since CNNs share parameters spatially (i.e., the same convolutional kernel is used to process all parts of the input), they typically need to learn a smaller number of parameters, which helps reduce overfitting of the model.

In the case of multivariate time-series data, CNNs are not only able to extract features in the time dimension, but also to reduce the correlation between time series. Therefore, if a forecasting model needs to consider multiple correlated time series simultaneously (e.g., various economic indicators or prices of other financial products), CNN-LSTM can effectively handle such ''multi-channel'' data.

IV. RESEARCH ON THE CHARACTERISTICS OF PRICE FLUCTUATIONS AND INFLUENCING FACTORS OF NON-FERROUS COPPER METAL

In this section, we examine the characteristics of fluctuations in copper prices and explore their historical trends in the international market. We analyze various factors that may impact copper price fluctuations, including the fundamental supply and demand relationship, energy costs, competition from alternative metals, global macroeconomic conditions, national policies, and other uncertainties.

A. PRICE FLUCTUATION CHARACTERISTICS OF NON-FERROUS COPPER METAL

Non-ferrous copper metal is a crucial strategic resource that finds widespread use in industries such as power electronics, machinery manufacturing, energy construction, transportation, military manufacturing, and aviation equipment. Furthermore, since the establishment of copper futures trading by the London Metal Exchange (LME) in 1877, the role of copper as a bulk commodity in the financial market has become increasingly prominent.

Non-ferrous copper possesses dual attributes as both an inherent commodity and a financial instrument that can be used to hedge against inflation through futures trading. Therefore, when studying the price fluctuations of copper, it is crucial to consider not only the primary supply and demand relationship in the market but also the influence of its financial attributes.

The non-ferrous copper metal's commodity properties are its essential attributes and play a crucial role in determining its medium and long-term price trends. Copper prices are influenced by global supply and demand factors. When the demand for copper exceeds its supply, market forces drive copper prices upward, while the opposite occurs when supply outstrips demand, causing prices to fall. Over time, fluctuations in copper prices can also affect the supply and demand of copper in the market. A decrease in copper prices leads to an increase in demand while the available stock decreases, and vice versa. This process gradually adjusts the supply and demand balance until the copper price stabilizes, reflecting the equilibrium in the market.

Financial attributes are secondary characteristics of non-ferrous copper. With the increasing financialization of the futures market, the economic properties of copper as a futures commodity have become more prominent. The financial attributes of copper stem from its nature as an asset that can be used to preserve and increase value by linking it to exchange rates and consumption indices. Moreover, copper can serve as a financing tool. Thanks to its high unit value, high density, ease of storage, and liquidity, copper, as a non-renewable resource, is useful in the financial sector through warehouse receipt pledges and trade financing, among other applications.

To summarize, several uncertain factors influence the market price of copper, and its price fluctuations have no apparent pattern. The combined effect of multiple complex factors generates non-cyclical, non-linear, frequent, and volatile changes. Fig. 3 illustrates the daily closing price fluctuations of LME copper from July 7, 2008, to October 29, 2021, using the corresponding data.

Fig. 3 depicts the historical fluctuations of copper prices over the past 13 years, where the lowest price was less than

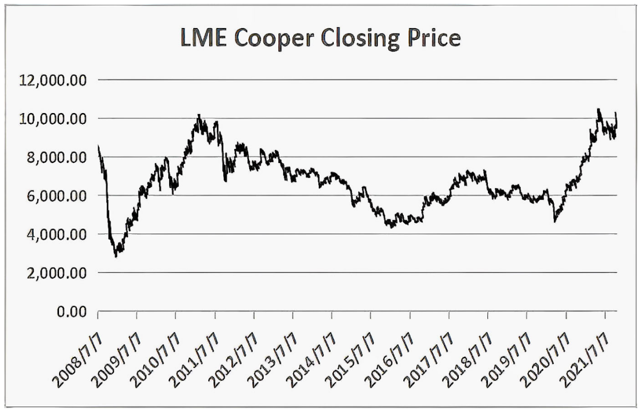

FIGURE 3. LME copper closing price from July 7, 2008, to October 29, 2021.

\$3,000 per ton, and the highest exceeded \$10,000 per ton, showing significant and unpredictable variations. Notably, copper price changes can be roughly divided into four stages: (1) During 2008-2009, the global financial crisis, triggered by the U.S. subprime mortgage crisis, led to a sharp decline in copper prices; (2) From 2009 to 2011, efforts by the Chinese and U.S. governments to counter the economic downturn drove the global economic recovery, resulting in a surge in copper prices; (3) Between 2011 and 2020, with the easing of monetary policies worldwide, bulk commodities gradually gained appeal among investors as an asset class, thereby highlighting the financial attributes of copper; (4) From 2020 to the present, the COVID-19 pandemic has significantly impacted copper prices, which initially declined before slowly bouncing back due to the vaccine's introduction and broader epidemic mitigation measures.

B. STUDY ON FACTORS INFLUENCING PRICES OF NON-FERROUS COPPER METALS

The previous examination of historical trends in LME copper closing prices reveals that prices continue to fluctuate due to a confluence of complex factors. This subsection will explore copper price fluctuations within the context of various uncertainties, including but not limited to supply and demand dynamics, energy costs, alternative metals, global macroeconomic conditions, and national policies.

1) SUPPLY AND DEMAND

As noted earlier, non-ferrous metals, including copper, are commodity assets whose medium and long-term trends are primarily determined by supply and demand dynamics.

2) ENERGY COSTS

The price fluctuations of copper are significantly influenced by the energy cost required in its smelting process, with the likes of oil and natural gas [33] playing pivotal roles. Currently, the pyrometallurgical method is predominantly used in copper smelting, with oil and natural gas serving as crucial raw materials and fuels throughout the process.

Consequently, energy expenses also exert significant pressure on copper prices.

3) ALTERNATIVE METALS

Non-ferrous metals, such as zinc and aluminum, can serve as potential substitutes for copper in certain applications. If the price gap between copper and these metals widens beyond a certain limit, some demand for copper may shift to alternatives like aluminum or zinc, resulting in lower market demand for copper and ultimately leading to a corresponding reduction in copper prices. Furthermore, copper is often preferred over precious metals like gold and silver due to its lower cost and greater availability. In certain situations, copper can also replace gold and silver [34]. Therefore, fluctuations in gold and silver prices can marginally impact copper demand in the market, thereby affecting copper prices as well.

4) GLOBAL MACROECONOMIC CONDITIONS

Global economic conditions have a significant bearing on the performance of relevant companies and economies, leading to fluctuations in international copper prices that are closely tied to industrial consumption demand [18], [35]. During periods of a weak global macroeconomic environment or financial crisis, the prices of international copper tend to decline, while an optimistic global economic outlook usually drives international copper prices upward.

Moreover, the international copper market typically employs the U.S. dollar as the trading currency. A surge in the dollar index suggests that the value of the dollar has risen, which results in a reduction in purchasing power and ultimately leads to a corresponding drop in copper prices. Conversely, a fall in the dollar index is likely to spur an increase in purchasing power, which stimulates demand and subsequently leads to a rise in copper prices. Therefore, there exists an inverse relationship between the dollar index and the trend of copper prices.

5) NATIONAL POLICIES AND OTHER UNCERTAINTIES

Significant policy changes in major copper-producing and consuming countries can also have a considerable impact on copper prices. For instance, in 2015, China incentivized the use of copper scrap as a raw material, leading to an increase in copper scrap imports. However, in 2017, to mitigate the adverse environmental impact of hazardous solid waste, China enforced restrictions on copper scrap imports. Consequently, the amount of copper scrap imports had a direct impact on the fluctuations in copper prices.

To sum up, the fluctuations in copper prices are influenced by a multitude of factors, including but not limited to the supply and demand dynamics of copper in the international market, energy costs, the availability of alternative metals, global macroeconomic conditions, and significant policy changes in major copper-producing and consuming countries. These complex and interrelated factors impact copper prices to varying degrees.

V. THE CHOICE OF NON-FERROUS METAL PRICE INFLUENCING FACTORS

As described above, the closing price fluctuations of copper are primarily driven by uncertain factors such as the supply and demand dynamics of copper in the market, energy costs associated with copper smelting, the availability of alternative metals, global macroeconomic conditions, and national policies. Furthermore, these factors are becoming increasingly interconnected, leading to a more intricate relationship between them.

This section examines various factors that can impact fluctuations in copper supply and demand, including refined copper production, inventory, and consumption. We also consider energy costs by analyzing WTI crude oil futures and natural gas futures, and assess the influence of alternative metals using gold futures, silver futures, and zinc futures. To gauge global macroeconomic conditions, we analyze the Dow Jones Industrial Average (DJI), NASDAQ, S&P 500 (SPX), and the U.S. dollar index. In addition, we investigate national policies and other uncertainties by selecting Chinese copper scrap imports, U.S. C-coffee futures, U.S. soybean futures, and lean hog futures as explanatory variables for predicting non-ferrous copper metal closing prices. Historical international copper closing prices ($/ton) are combined with these factors to predict future copper prices.

Table 1 presents the 16 selected factors that impact copper price fluctuations, categorized into five perspectives, and are used as explanatory variables in our copper price prediction model. We obtained data on refined copper production, inventory, and consumption from the International Copper Study Group (ICSG), while data on copper scrap imports were collected from the General Administration of Customs of China. The remaining futures and index data were sourced from the Invesco website, and all variables are reported monthly.

To comprehensively characterize the factors influencing copper closing prices, it is crucial to select an adequate number of feature variables. However, including too many feature variables can lead to redundant information and increased complexity. Each feature variable is complex and interacts with others, further compounding this complexity. This high level of complexity can lead to overfitting during the training process, leading to decreased generalization performance of the prediction model. Therefore, it is important to strike a balance between selecting enough feature variables to capture the relevant factors and keeping the model simple enough to prevent overfitting.

The accuracy of the deep learning model used in this study is heavily reliant on the quality of the input feature information. To ensure the generalization and precision of the prediction model, the multidimensional features selected above undergo a thorough analysis and processing. Firstly, we qualitatively analyze the correlation between each influencing factor and international copper prices by analyzing scatter plots. Next, we use the Pearson correlation coefficient to quantitatively assess the correlation between each influencing factor and international copper prices. We then exclude

TABLE 1. (a) Copper price volatility influencing factors data. (b) Copper price volatility influencing factors data.

(a)

Date	Supply and demand			Energy costs		Alternative metals		
	Refined copper production (kiloton)	Refined coppe inventory (kiloton)	Refined coppe consumption (kiloton)	WTI crude oil futures (USD/bbl)	Natural gas futures (USD/1000m3)	Gold futures (USD/oz)	Silver futures (USD/oz)	Zinc futures (USD/ton)
2011.03	1352	1387	1617	106.72	4.389	1,439.90	37.9	2,360
2011.04	1276	1391	1583	113.93	4.698	1,557.00	48.599	2,259
2011.05	1348	1311	1723	102.7	4.666	1,536.80	38.317	2,265
…	…	…	…	…	…	…	…	…
2021.08	1757	1415	2039	68.5	4.377	1,816.90	23.991	3,003.50
2021.09	1734	1300	2121	75.03	5.867	1,757.00	22.047	2,988.00
2021.10	1747	1287	2147	83.57	5.426	1,784.90	23.966	3,378.50

(b)

Date	Global macroeconomic conditions				National policies and other uncertainties			
	DJI	NASDAQ	S&P 500	U.S. dollar index	Chinese copper scrap imports (million tons)	U.S. C-coffee futures (USD/lb)	Soybean futures (USD/bushel)	Lean hog futures (USD/lb)
2011.03	12,319.73	2,338.99	12,319.73	2,338.99	12,319.73	2,338.99	12,319.73	2,338.99
2011.04	12,810.54	2,404.08	12,810.54	2,404.08	12,810.54	2,404.08	12,810.54	2,404.08
2011.05	12,569.79	2,372.54	12,569.79	2,372.54	12,569.79	2,372.54	12,569.79	2,372.54
…	…	…	…	…	…	…	…	…
2021.08	35,360.73	15,582.51	35,360.73	15,582.51	35,360.73	15,582.51	35,360.73	15,582.51
2021.09	33,843.92	14,689.62	33,843.92	14,689.62	33,843.92	14,689.62	33,843.92	14,689.62
2021.10	35,819.56	15,850.47	35,819.56	15,850.47	35,819.56	15,850.47	35,819.56	15,850.47

features with weak correlation and only select explanatory variables with a strong correlation with global copper prices. This screening process ensures accurate prediction of copper prices by using the most relevant and influential factors.

A. SCATTER PLOT CORRELATION ANALYSIS

By observing the distribution of data points in the scatter plot of copper prices and various factors, we can qualitatively analyze the correlation between each factor and copper prices.

Fig. 4 displays the scatter plot of the initial selection of influencing factors in Table 1, along with international copper prices.

In Fig. 4(a), we observe a negative correlation between refined copper production and international copper prices in the range of 1200-1500 kt. When the production of refined copper increases, the supply of copper in the market also increases, resulting in a decline in international copper prices. However, when refined copper production exceeds 1500 kt, the global copper price no longer decreases. This is because the decrease in copper price leads to increased demand in the market, eventually resulting in a balance in supply and demand, keeping the copper price floating between 4000-8000 USD/ton. Fig. 4(b) shows a negative correlation between the amount of refined copper inventory and international copper prices. An increase in refined copper inventory indicates that the production in the market is greater than the current consumption. The excess supply of copper in the market leads to a decline in copper prices. Finally, in Fig. 4(c), we can see that consumption of refined copper in the range of 1500-1900 kt also negatively correlates with international copper prices. A high international copper price stimulates the expansion of copper production capacity, leading to an increase in copper supply on the market, and a resulting decline in copper price. As the copper price drops to a certain range, the demand for copper increases, and ultimately, the market reaches a state of balance between supply and demand, which stabilizes the copper price.

Fig. 4(d) and Fig. 4(e) demonstrate a positive correlation between WTI crude oil and natural gas futures with international copper prices. The smelting process requires heavy oil and natural gas to fuel the equipment and LPG as a raw material during the reduction period, making crude oil and natural gas energy sources essential for the copper smelting industry. Moreover, crude oil and natural gas are critical industrial raw materials, and their price fluctuations can reflect the global economic situation to some extent. So, when the international crude oil and natural gas prices rise, it leads to corresponding adjustments in copper prices.

Fig. 4(f), Fig. 4(g), and Fig. 4(h) demonstrate a positive correlation between gold, silver, and zinc prices with international copper prices. Copper is often used interchangeably with gold and zinc in certain products. As a result, an increase in the cost of gold and silver may cause some of the demand to shift towards copper, leading to an upward trend in copper prices. Similarly, an increase in zinc prices may also cause a rise in copper prices to some extent.

The Dow Jones Industrial Average (DJI), NASDAQ, and the S&P 500 are three crucial stock market indices in the US that can reflect the global economic situation. To examine their correlation to the international copper price, we selected the DJI index, and Fig. 4(i) shows its non-monotonic correlation with global copper price. The Dow Jones index continues to rise continuously by updating its constituents regularly, while the international copper price has been fluctuating over the past decade due to several complex factors such as national policies and epidemics. Therefore, the expected correlation between the three indices and the international copper price is less pronounced than predicted.

Fig. 4(l) illustrates that the U.S. dollar index has a negative correlation with international copper prices. An increase in the dollar index indicates an appreciation of the dollar, which causes non-US buyers to spend more in their currency to purchase the same amount of copper leading to a decrease in demand and purchasing power, ultimately causing a decline in international copper prices. Conversely, a decrease in the dollar index represents a depreciation of the dollar, increasing the purchasing power and demand, ultimately leading to an increase in international copper prices.

Fig. 4(m) reveals that the correlation between copper scrap imports and international copper prices is not significant. This outcome is mainly due to China's national grid renovation and waste appliance dismantling programs, which have generated significant quantities of copper scrap. This copper scrap has filled the gap in copper scrap demand, resulting in minimal impact on international copper prices.

Furthermore, as revealed in Fig. 4(n), Fig. 4(o), and Fig. 4(p), coffee futures, soybean futures, and lean hog futures all have a positive correlation with international copper prices. This is due to the fact that in relatively mature futures markets, if the prices of these critical commodities futures (coffee, soybean, and lean pork) show an upward trend, it indicates a better development of the real economy. Consequently, the demand for copper increases, leading to a change in supply and demand ultimately resulting in an increase in copper prices.

B. PEARSON COEFFICIENT CORRELATION ANALYSIS

To analyze the correlation between copper prices and various influencing factors, we employed the Pearson correlation coefficient method [36]. This method quantitatively analyzes the correlation among variables based on their covariance and standard deviation. For instance, to examine the relationship between copper prices and the closing price of gold, we calculated the correlation coefficient using the following formula.

$$\rho_{c,g} = \frac{cov(P_c, P_g)}{\sigma_{P_c} \times \sigma_{P_g}} \tag{9}$$

where c and g indicate Copper and Gold, P_c and P_g show the closing price of copper and gold, $cov(P_c, P_g)$ means the covariance of copper and gold prices, and $\sigma_{P_c}$and σ_{P_g} indicate the standard deviation of copper and gold prices. $\rho_{c,g}$ shows the correlation coefficient between copper and gold prices. The covariance of gold and copper prices is calculated as

$$cov(P_c, P_g) = \frac{1}{n}\sum_{i=1}^{n}(P_{ci} - \overline{P_c})(P_{si} - \overline{P_s}) \tag{10}$$

where n is the total number of samples, P_{ci} and P_{si} is the copper and gold prices at the i-th sample point, respectively, and $\overline{P_c}$ and $\overline{P_c}$ are the average values of copper and gold prices, respectively.

TABLE 2. Pearson correlation coefficients between copper price influencing factors and copper prices.

Influencing factor	Correlation coefficient	Correlation Strength
copper production	-0.304	weak
copper inventory	-0.298	weak
copper Consumption	-0.279	weak
WTI crude oil	0.655	strong
natural gas futures	0.526	medium
gold price	0.623	strong
silver price	0.778	strong
zinc price	0.277	weak
DJI	0.045	no
NASDAQ	0.164	no
the S&P 500	0.067	no
dollar index	0.671	strong
copper scrap imports	0.179	no
coffee futures	0.595	medium
soybean futures	0.741	strong
lean hog futures	0.575	medium

If the Pearson correlation coefficient is zero, it indicates that there is no correlation between copper price and gold price. A positive number between (0, 1] implies a positive correlation between copper price and gold price, with a higher value indicating a stronger correlation. Conversely, a negative number between [-1, 0) suggests a negative correlation between copper price and gold price, with a smaller value indicating a stronger negative correlation. We categorized the correlation between variables into five groups based on the magnitude of Pearson's correlation coefficient: no correlation, weak correlation, moderate correlation, strong correlation, and very strong correlation.

To examine the correlation between each influencing factor and global copper price, we calculated the Pearson correlation coefficient between each variable and copper price and gave the correlation strengths. Table 2 illustrates the Pearson correlation coefficients between worldwide copper price and each influencing factor.

Table 2 displays the correlation coefficients between international copper prices and each influencing factor. Our analysis revealed that factors such as refined copper production, inventory, and consumption - selected from the supply and demand perspective - displayed weak correlation with global copper prices. On the other hand, WTI crude oil and natural gas - selected from the energy cost perspective - moderately and strongly correlate with international copper prices, respectively. Gold and silver, chosen from the perspective of alternative metals, exhibit a strong correlation with international copper prices, while zinc displays a weak correlation. In terms of global macroeconomic perspective, the Dow Jones Index, NASDAQ Index, and S&P 500 Index do not correlate with copper prices and have little influence on them; thus, we excluded these three factors. The U.S. dollar index is highly correlated with international copper prices. Furthermore, while the correlation between China's copper scrap imports and international copper prices - selected from

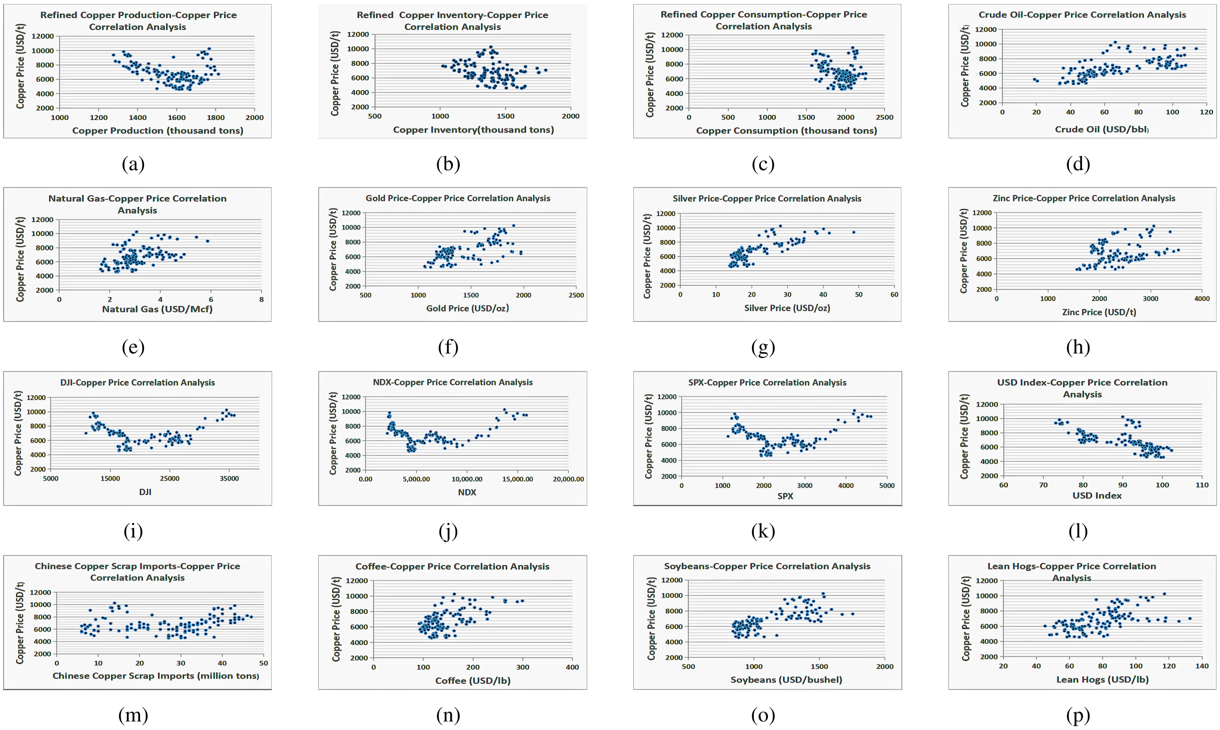

FIGURE 4. Correlation analysis between influencing factors and copper prices.

the national policy perspective - is less than 0.2, we still discarded it. Finally, coffee, soybean, and lean pork futures show moderate-to-strong correlation with international copper prices, respectively.

Table 2 focuses solely on the degree of influence of each factor on international copper prices, while disregarding the correlation between these factors. Although Table 2 partially eliminates redundant information, further refinement is necessary. We need to conduct two more screening processes by analyzing the correlation coefficients between each influencing factor to obtain a more accurate analysis.

After the first screening, a heat map in Fig. 5 illustrates the Pearson correlation coefficients between each influencing factor. The coordinate values 1 to 12 in Fig. 5 correspond to Copper Production, Copper Inventory, Copper Consumption, Crude Oil, Natural Gas, Gold, Silver, Zinc, USD Index, Coffee, Soybean, and Lean Hogs, respectively.

In Fig. 5, the right side of the heat map displays the color index and the squares record the correlation coefficients between each influencing factor. Based on the correlation coefficients calculated in Fig. 4 and the Pearson correlation criteria analysis in Table 2, we can observe that the correlation coefficient between WTI crude oil and the U.S. dollar index is -0.89, indicating a very strong correlation that enhances redundancy in the data set. Although the correlation indices of WTI crude oil, the U.S. dollar index, and international copper price are 0.655 and 0.671, respectively, WTI crude oil has a lesser influence on global copper prices than the U.S.

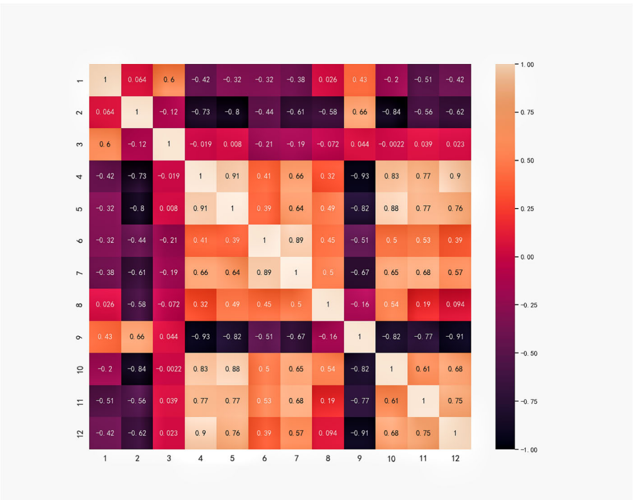

FIGURE 5. Pearson correlation coefficient heat map.

dollar index. Therefore, we exclude WTI crude oil from our analysis.

To summarize, we have selected refined copper production, copper stocks, copper consumption, natural gas, gold, silver, zinc, the U.S. dollar index, coffee, soybeans, and lean hogs as the final set of influencing factors. The process of filtering these 11 factors effectively reduces redundancy in the dataset and maximizes its information integrity. This will decrease the training cost of the prediction model and improve its accuracy in predicting future trends.

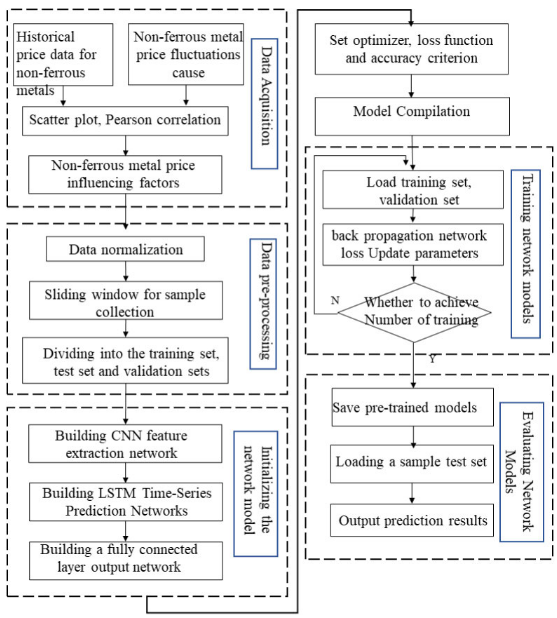

FIGURE 6. General flowchart of multi-influencing copper price prediction based on CNN-LSTM.

VI. CNN-LSTM-BASED MONTHLY PRICE PREDICTION MODEL

A. OVERALL SYSTEM FLOW CHART

The general flow of CNN-LSTM-based multi-influencing factor price prediction proposed in this paper is shown in following Fig. 6.

The proposed multi-influencing factor price prediction using CNN-LSTM follows a general flow consisting of two phases. In the first phase, data acquisition is performed where we select main influencing factors using scatter plots and Pearson correlation coefficients as discussed in Section V. In the second phase, the collected data is pre-processed and sent to CNN-LSTM to train the model parameters.

B. INPUT DATA PRE-PROCESSING

Table 1 presents the dataset information utilized in this study, where copper prices and their respective influencing factors exhibit different magnitudes. To ensure compatibility among the various dimensions of the dataset during training of the CNN-LSTM prediction model, normalization is necessary. In this paper, we employ a normalization method, which involves:

$$x_t^* = \frac{x_t - x_{min}}{x_{max} - x_{min}} \tag{11}$$

where x_t denotes the original data before normalization, x_{max} and x_{min} are the maximum and minimum values in the sequence, respectively, and x_t^* denotes the normalized data with values between 0 and 1

Upon completion of dataset normalization, it is necessary to adjust the dataset format in accordance with the internal structure of the network. This conversion is carried out by sliding window and sliding step sampling, resulting in a [TIME_STEP, INPUT_FEATURES] format. Here, TIME_STEP represents the input data step size for consecutive data points, while INPUT_FEATURES indicates the feature dimension of the input data. In essence, a sliding window size of TIME_STEP is employed to sample the time dimension, using the data of the first TIME_STEP month as input and copper price of the subsequent month (TIME_STEP+1) as output.

Subsequently, the sample set obtained through sliding window sampling is further divided into a training set, validation set, and test set. This division is necessary to enable adequate training and evaluation of the prediction model on a specified scale.

C. NETWORK TRAINING PROCESS

The network training module in the model includes three parts: the network initialization module, the network training module and the network evaluation module.

1) THE NETWORK INITIALIZATION MODULE

This module comprises of three parts, namely the CNN network, the LSTM network, and the fully connected network. The primary function of the CNN network is to extract features from multi-dimensional data, while the LSTM network extracts information from the time dimension. Finally, prediction information is output through the fully connected network. During network initialization, several hyperparameters such as the number of convolutional kernels, convolutional kernel size, filter size of the CNN network, number of cells in the LSTM network, and the fully connected layer must be defined.

2) THE NETWORK TRAINING MODULE

Once the network model has been initialized, the next step involves setting the optimizer, loss function, and accuracy criterion to compile the model. This is followed by inputting the training and validation sets, and continuously optimizing the network parameters.

3) THE NETWORK EVALUATION MODULE

In order to examine the accuracy and validity of the prediction model, we feed the test set samples into the pre-trained model and evaluate its performance using various metrics.

D. PSEUDO-CODE FLOW

The pseudo-code flow of the proposed CNN-LSTM-based price prediction method is as follows:

VII. EXPERIMENTAL VALIDATION ANALYSIS

A. DESCRIPTION OF THE EXPERIMENTAL DATA SET

As mentioned earlier, the initially identified factors influencing copper price fluctuations in Table 1 underwent two rounds of screening to finalize the list of influencing factors. Based on this, we selected the international copper prices

TABLE 3. The pseudo-code flow of the proposed CNN-LSTM-based price prediction method.

Data Collection:
Inputting non-ferrous historical price data and influencing factor data
Outputting scatter plot, Pearson correlation coefficient table and heat map
Determination of non-ferrous metal price influencing factors and complete data collection
Data pre-processing:
Standardization of data sets
Sliding window to collect samples
Segmentation of training, validation and test sets
The network initialization module:
Construction of CNN feature extraction network
Constructing LSTM temporal prediction network
Building a fully connected output network
The network training module:
Loading training set and validation set
Calculating the error of the network layers and back-propagating to update the network parameters
Saving the pre-trained model
The network evaluation module:
Loading the test set
Outputting prediction results

and related factors from March 2011 to June 2021 to form the dataset used in this study. The data is structured as (124, 12), consisting of 124 sampling points and 12 characteristic columns. Fig. 7 depicts the dataset of international copper prices and related influencing factors.

We partitioned the dataset into training, validation, and test sets according to a 6:2:2 ratio. Subsequently, we used sliding window sampling with a window width of 7 and a step size of 1 to intercept data from the previous seven months of copper price and associated influencing factors, and predict the copper price for the eighth month. The sampled training set, validation set, and test set are structured as (69, 7, 12), (17, 7, 12), and (17, 7, 12) respectively, while the output formats are (69, 1), (17, 1), and (17, 1) respectively.

B. EXPERIMENTAL EVALUATION METRICS

To evaluate the accuracy of the prediction model, we selected root mean square error (RMSE), mean absolute error (MAE) and mean absolute percentage error (MAPE) for evaluation in this paper. The formulas for these three evaluation metrics are as followings:

$$RMSE = \sqrt{\frac{1}{m}\sum_{i=1}^{m}(R_i - P_i)^2} \tag{12}$$

$$MAE = \frac{1}{m}\sum_{i=1}^{m}|R_i - P_i| \tag{13}$$

$$MAPE = \frac{1}{m}\sum_{i=1}^{m}|\frac{R_i - P_i}{R_i}| \tag{14}$$

where R_i denotes the actual copper price in the i-th week, P_i denotes the copper price forecast result in the i-th week, and m denotes the number of forecast samples. All three indicators are used to assess the accuracy of the forecasting model, reflecting the difference between the predicted copper price and the actual copper price. The smaller the value, the better the forecasting result.

TABLE 4. Prediction results with different numbers of network layers.

Number of convolution layers	Number of pooling layers	Number of LSTM layers	RMSE
1	1	1	49.44
1	1	2	39.50
1	1	3	33.54
1	1	4	37.74
2	1	3	30.13
3	1	3	37.50
2	2	3	32.19

C. EXPERIMENTAL PARAMETER SETTING

The hyperparameters set for the proposed CNN-LSTM network in this study consists of two main parts. The first set includes hyperparameters such as the number of layers and neurons in the CNN and LSTM. The second set includes hyperparameters such as loss function, optimizer, learning rate, and the number of training sessions required for model training.

1) NUMBER OF NETWORK LAYERS

The performance of a deep neural network model is closely linked to the number of network layers. Generally speaking, increasing the number of layers can enhance the model's processing power to a certain extent. However, the predictive power of the model does not always improve linearly with the number of network layers. With each additional layer, the complex structure of the neural network significantly increases the model's training time and internal parameters. Moreover, overfitting may occur due to an excessive number of layers. Therefore, in this study, we determined the optimal number of network layers for the prediction model by comparing the RMSE values of model predictions under different neural network layer configurations, as shown in Table 4. Table 4 displays some of the prediction results obtained using different network layers. From the first four rows of the table, it is clear that the RMSE value decreases as the number of LSTM layers increases when the number of LSTM layers is less than 3. Nonetheless, if we continue to increase the number of LSTM layers, it would eventually lead to an increase in the RMSE value, and the model performs optimally when it has 3 LSTM layers. Similarly, upon observing the data in rows 5, 6, and 5, 7, we can conclude that the model has a minor prediction error when configured with two convolutional layers and one pooling layer. As such, we finalized the model structure as having two convolutional layers, one pooling layer, and three LSTM layers.

2) NUMBER OF NEURONS

The model's prediction accuracy is also influenced by the number of neurons in the neural network. Within a certain range, increasing the number of neurons can enhance the

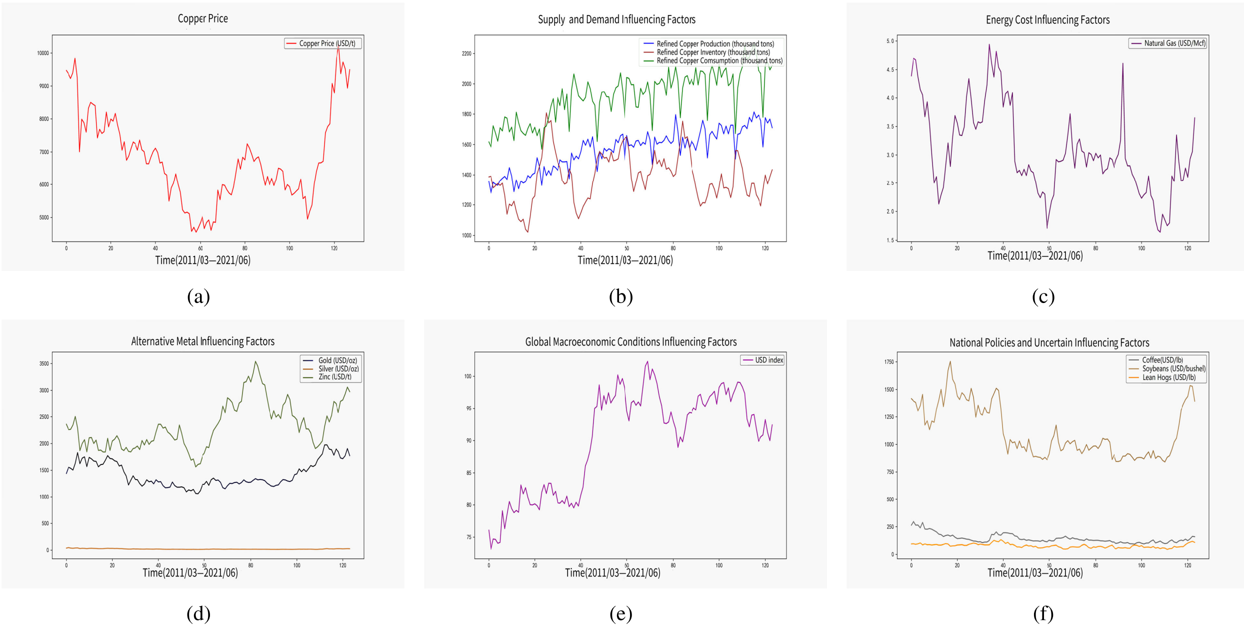

FIGURE 7. The dataset of international copper prices and related influencing factors.

TABLE 5. The number of neurons corresponding to different network layers.

Network layer	The number of neurons
Layer 1 convolutional layer	filters:128,kernel_size:3
Layer 2 convolutional layer	filters:64,kernel_size:2
Pooling layer	pool_size:2
Layer 1 LSTM	units:128
Layer 2 LSTM	units:128
Layer 3 LSTM	units:128

speed and precision of model training. However, beyond this range, increasing the number of neurons would result in poor training outcomes. Therefore, in this study, we initially set the number of neurons according to an empirical formula and then fine-tuned it through experiments. The final selected neuron hyperparameters are presented in Table 5.

3) THE LOSS FUNCTION

The loss function is a metric utilized to assess the disparity between the predicted values and actual values during the training phase. The model's prediction accuracy is deemed superior with a lower loss function. In this study, we employed the mean squared error (MSE) as the loss function, which is suitable for resolving regression problems. The calculation of the MSE value can be expressed by the following formula:

$$MSE = \frac{1}{m}\sum_{i=1}^{m}(R_i - P_i)^2 \tag{15}$$

The symbols in Eq. (15) are the same as those in Eq. (12) - Eq. (14).

4) OPTIMIZER AND LEARNING RATE

During backpropagation, the optimizer continuously tunes the optimization model's parameters to minimize the loss function and decrease the gap between the predicted results and actual values. This process enables the updated model to achieve a global optimum prediction effect. The learning rate serves as the basis for dynamically adjusting the weight and bias size at each training session, and its value influences the convergence speed and accuracy of the model. A low learning rate leads to small adjustment magnitudes, thereby lengthening the model's training time and convergence duration. Conversely, a high learning rate results in significant adjustment magnitudes, causing the model to oscillate repeatedly around the optimal value and reducing the model's prediction accuracy. In this study, we employed the Adam optimizer [37], which can automatically adjust the learning rate. We set the initial value of the learning rate to $1 \times e^{-3}$ based on empirical methods.

5) NUMBER OF MODEL TRAINING

The number of training iterations also has an impact on the prediction performance of the model. In theory, increasing the number of training iterations raises the likelihood of the loss function achieving the optimal value. Nonetheless, when the number of training iterations is excessively high, it can result in overfitting of the model, causing the prediction model to perform well on the training set but poorly on the validation and test sets, thereby affecting the model's generalization. In this study, we set the number of training epochs to 100 and the batch size to 4 based on empirical methods and the results of numerous experiments. These parameters were chosen to strike a balance between improving the model's convergence rate and avoiding overfitting.

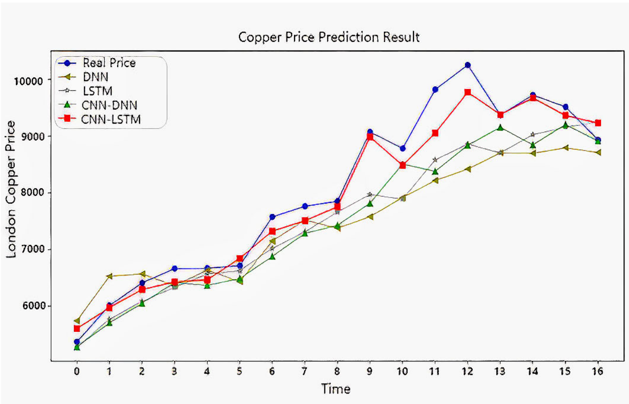

FIGURE 8. Copper price forecast results under multiple influencing factors.

D. ANALYSIS OF EXPERIMENTAL RESULTS

To evaluate the CNN-LSTM price prediction method's efficiency and stability under various influencing factors proposed in this research, we conducted comparative experiments with other models such as Deep Neural Network (DNN), LSTM, and mixed-model CNN-DNN network. The experimental results of these four prediction models are presented in Fig. 8.

According to Fig. 8, the DNN network is somewhat close to the actual value for certain data points in copper price prediction. However, most of the observations deviate from the true values, indicating that the simple DNN network is inadequate for addressing intricate time-series data prediction problems. In contrast, the LSTM network is more precise in predicting the copper price fluctuation trends owing to its superior time-series data processing capabilities. Nevertheless, the LSTM network alone is insufficient for effectively extracting the spatial feature information of the multi-dimensional dataset, resulting in notable inaccuracies in prediction accuracy.

The proposed CNN-LSTM model in this research significantly reduces the amount of data and number of parameters transmitted in the network after conducting spatial dimension feature extraction and data dimensionality reduction of copper price and influencing factor data by CNN network. Consequently, the LSTM network's time-series feature extraction capabilities are amplified, resulting in a considerable improvement in the model's prediction abilities. Upon observing the fluctuation curves of the CNN-LSTM network's prediction results and actual prices, we can note some errors between certain data points of the predictions and the actual values. Despite this, the overall prediction accuracy and fluctuation trends of the CNN-LSTM network are the most well-fitted.

Fig. 9. shows the results of comparing different models' forecasting performance evaluation indexes.

The CNN-LSTM method proposed in this research outperforms all other prediction models in terms of the three metrics, namely RMSE, MAE, and MAPE. For single-model prediction, the LSTM model has lower error values than the DNN model due to the former's capacity to capture medium- and long-term dependencies of intricate time series. Moreover, after adding the CNN feature extraction network, the prediction errors of both the CNN-DNN network and the CNN-LSTM network are lower than those of their respective single models. Out of all models, the CNN-LSTM network proposed in this research yields the lowest prediction error value.

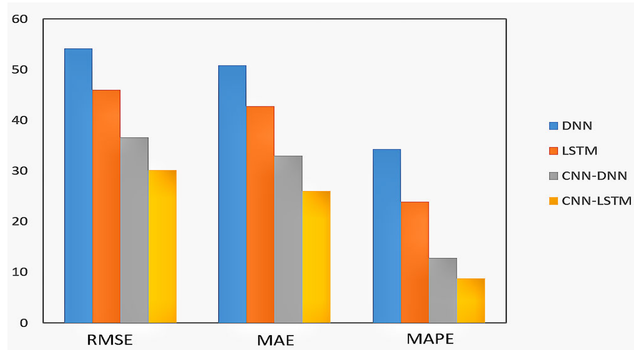

FIGURE 9. Comparison of RMSE, MAE and MAPE metrics of different models.

TABLE 6. Comparison of the errors of different copper price forecasting models.

Models	RMSE	MAE	MAPE	RMSE
DNN	54.16	50.83	34.28	54.16
LSTM	46.03	42.77	23.91	46.03
CNN-DNN	36.62	33.01	12.80	36.62
CNN-LSTM	**30.13**	**26.02**	**8.82**	**30.13**

The above conclusion is deduced from Fig.9. Table 6 displays the quantitative analysis of the model's prediction accuracy, presenting the RMSE, MAE, and MAPE results of all four methods.

Table 6 reveals that the CNN-LSTM model proposed in this research yields the lowest values for all three metrics, namely RMSE (30.132), MAE (26.020), and MAPE (8.819). Hence, the proposed method demonstrates the most exceptional prediction performance among all other models.

When considering single-model prediction methods, the DNN approach yields inferior results for all three metrics (RMSE: 54.16, MAE: 50.29, and MAPE: 34.28) in comparison to LSTM due to its reduced effectiveness in managing time-series data. However, LSTM demonstrates promising potential in processing time series as demonstrated by its superior performance, with RMSE, MAE, and MAPE values of 46.03, 42.77, and 23.91 respectively, resulting in improvements of 15.02%, 15.85%, and 30.26% relative to DNN. By incorporating CNN networks to extract dimensional spatial features, both CNN-DNN and CNN-LSTM models present substantially better performance with all three metrics (RMSE: 36.62, MAE: 33.01, and MAPE: 12.80 and RMSE: 30.13, MAE: 26.02, and MAPE: 8.82, respectively), leading to an improvement of 32.39%, 35.05%, 62.66%, and 34.54%, 39.17%, 63.11%, respectively, compared to the single model. This is due to the ability of CNN networks to extract spatial features and perform deep mining of features between copper prices and influencing factors, demonstrating that the incorporation of CNN can further enhance model performance.

VIII. CONCLUSION

This paper primarily addresses the price forecasting problem of non-ferrous metals under multiple influencing factors. To tackle this problem, the study selects refined copper production, inventory, and consumption, natural gas, gold, silver, zinc, U.S. dollar index, coffee, soybean, and lean pork as contributing factors to copper prices. Additionally, we propose a CNN-LSTM monthly price forecasting model. Through experimental validation and analysis, our findings indicate that compared to DNN and LSTM networks, our proposed CNN-LSTM method outperforms in terms of both forecasting accuracy and trend-fitting results.

The follow-up work focuses on continuous refinement and supplementation of the algorithm, as follows:

1) The monthly price forecasting model exhibits limited generalization abilities due to the rapidly changing nature of the free market. Unexpected significant events, such as economic crises or pandemics, can cause drastic and unpredictable fluctuations in copper prices. This leads to insufficient model generalization capacity. To address this issue, future research will undertake a more comprehensive and in-depth analysis of the factors associated with copper prices. We aim to leverage characteristic-rich information among influencing factors to accurately anticipate the future fluctuation trend of copper prices.
2) The fluctuations in historical copper price series are complex and volatile, presenting a wealth of feature-rich information. In future studies, we plan to explore various data mining algorithms to enhance the accuracy of our daily forecast model.

REFERENCES

[1] M. Zhong, R. He, J. Chen, and J. Huang, "Time-varying effects of international nonferrous metal price shocks on China's industrial economy," *Phys. A, Stat. Mech. Appl.*, vol. 528, Aug. 2019, Art. no. 121299.
[2] Q. Qu, L. Wang, Z. Cao, S. Zhong, C. Mou, Y. Sun, and C. Xiong, "Unfolding the price effects of non-ferrous industry chain on economic development: A case study of Yunnan province," *Resour. Policy*, vol. 61, pp. 1–20, Jun. 2019.
[3] X. Han, Z. Liu, and S. Wang, "An R-vine copula analysis of non-ferrous metal futures with application in value-at-risk forecasting," *J. Commodity Markets*, vol. 25, Mar. 2022, Art. no. 100188.
[4] R. J. Bianchi, J. H. Fan, and N. Todorova, "Financialization and de-financialization of commodity futures: A quantile regression approach," *Int. Rev. Financial Anal.*, vol. 68, Mar. 2020, Art. no. 101451.
[5] H.-J. Li and L. Wang, "Multi-scale asynchronous belief percolation model on multiplex networks," *New J. Phys.*, vol. 21, no. 1, Jan. 2019, Art. no. 015005.
[6] H. Li, Z. Bu, Z. Wang, J. Cao, and Y. Shi, "Enhance the performance of network computation by a tunable weighting strategy," *IEEE Trans. Emerg. Topics Comput. Intell.*, vol. 2, no. 3, pp. 214–223, Jun. 2018.
[7] H. Li, Z. Bu, A. Li, Z. Liu, and Y. Shi, "Fast and accurate mining the community structure: Integrating center locating and membership optimization," *IEEE Trans. Knowl. Data Eng.*, vol. 28, no. 9, pp. 2349–2362, Sep. 2016.
[8] G. P. E. Box and G. M. Jenkis, *Time Series Analysis: Forecasting and Control*. London, U.K.: Palgrave Macmillan, 2013, pp. 161–215.
[9] G. P. Zhang, "Time series forecasting using a hybrid ARIMA and neural network model," *Neurocomputing*, vol. 50, pp. 159–175, Jan. 2003.
[10] J. Contreras, R. Espinola, F. J. Nogales, and A. J. Conejo, "ARIMA models to predict next-day electricity prices," *IEEE Trans. Power Syst.*, vol. 18, no. 3, pp. 1014–1020, Aug. 2003.
[11] J. J. Reeves, "Bootstrap prediction intervals for ARCH models," *Int. J. Forecasting*, vol. 21, no. 2, pp. 237–248, Apr. 2005.
[12] H. Herwartz, "Stock return prediction under GARCH—An empirical assessment," *Int. J. Forecasting*, vol. 33, no. 3, pp. 569–580, Jul. 2017.
[13] D. García and W. Kristjanpoller, "An adaptive forecasting approach for copper price volatility through hybrid and non-hybrid models," *Appl. Soft Comput.*, vol. 74, pp. 466–478, Jan. 2019.
[14] E. Hadavandi, A. Ghanbari, and S. Abbasian-Naghneh, "Developing a time series model based on particle swarm optimization for gold price forecasting," in *Proc. 3rd Int. Conf. Bus. Intell. Financial Eng.*, Aug. 2010, pp. 337–340.
[15] L.-T. Zhao, G.-R. Zeng, L.-Y. He, and Y. Meng, "Forecasting short-term oil price with a generalised pattern matching model based on empirical genetic algorithm," *Comput. Econ.*, vol. 55, no. 4, pp. 1151–1169, Apr. 2020.
[16] Z. Alameer, M. A. Elaziz, A. A. Ewees, H. Ye, and Z. Jianhua, "Forecasting copper prices using hybrid adaptive neuro-fuzzy inference system and genetic algorithms," *Natural Resour. Res.*, vol. 28, no. 4, pp. 1385–1401, Mar. 2019.
[17] H. Dehghani and D. Bogdanovic, "Copper price estimation using bat algorithm," *Resour. Policy*, vol. 55, pp. 55–61, Mar. 2018.
[18] F. S. Lasheras, F. J. de Cos Juez, A. S. Sánchez, A. Krzemień, and P. R Fernández, "Forecasting the COMEX copper spot price by means of neural networks and ARIMA models," *Resour. Policy*, vol. 45, pp. 37–43, Sep. 2015.
[19] C. Ciner, "Predicting white metal prices by a commodity sensitive exchange rate," *Int. Rev. Financial Anal.*, vol. 52, pp. 309–315, Jul. 2017.
[20] J. A. Frankel and K. R. Andrew. (Sep. 2010). *Determinants of Agricultural and Mineral Commodity Prices*. [Online]. Available: https://research.hks.harvard.edu/publications/getFile.aspx?Id=609
[21] N. B. Behmiri and M. Manera, "The role of outliers and oil price shocks on volatility of metal prices," *Resour. Policy*, vol. 46, pp. 139–150, Dec. 2015.
[22] B. Mo, H. Nie, and Y. Jiang, "Dynamic linkages among the gold market, U.S. Dollar and crude oil market," *Phys. A, Stat. Mech. Appl.*, vol. 491, pp. 984–994, Feb. 2018.
[23] A. C. Ozdemir, K. Buluş, and K. Zor, "Medium- to long-term nickel price forecasting using LSTM and GRU networks," *Resour. Policy*, vol. 78, Sep. 2022, Art. no. 102906.
[24] D. Buncic and C. Moretto, "Forecasting copper prices with dynamic averaging and selection models," *North Amer. J. Econ. Finance*, vol. 33, pp. 1–38, Jul. 2015.
[25] G. Aye, R. Gupta, S. Hammoudeh, and W. J. Kim, "Forecasting the price of gold using dynamic model averaging," *Int. Rev. Financial Anal.*, vol. 41, pp. 257–266, Oct. 2015.
[26] C. Liu, Z. Hu, Y. Li, and S. Liu, "Forecasting copper prices by decision tree learning," *Resour. Policy*, vol. 52, pp. 427–434, Jun. 2017.
[27] J. D. Díaz, E. Hansen, and G. Cabrera, "A random walk through the trees: Forecasting copper prices using decision learning methods," *Resour. Policy*, vol. 69, Dec. 2020, Art. no. 101859.
[28] P. Zhang and B. Ci, "Deep belief network for gold price forecasting," *Resource Policy*, vol. 69, no. 10, pp. 1–10, Dec. 2020.
[29] Z. Alameer, M. A. Elaziz, A. A. Ewees, H. Ye, and Z. Jianhua, "Forecasting gold price fluctuations using improved multilayer perceptron neural network and whale optimization algorithm," *Resour. Policy*, vol. 61, pp. 250–260, Jun. 2019.
[30] H. Zhang, H. Nguyen, X.-N. Bui, B. Pradhan, N.-L. Mai, and D.-A. Vu, "Proposing two novel hybrid intelligence models for forecasting copper price based on extreme learning machine and meta-heuristic algorithms," *Resour. Policy*, vol. 73, Oct. 2021, Art. no. 102195.
[31] T. Kattenborn, J. Leitloff, F. Schiefer, and S. Hinz, "Review on convolutional neural networks (CNN) in vegetation remote sensing," *ISPRS J. Photogramm. Remote Sens.*, vol. 173, pp. 24–49, Mar. 2021.
[32] S. Hochreiter and J. Schmidhuber, "Long short-term memory," *Neural Comput.*, vol. 9, no. 8, pp. 1735–1780, Nov. 1997.
[33] K. J. A. Kundig and G. Joseph, *Copper: Its Trade Manufacture, Use, and Environmental Status*. OH, USA: ASM International, 1999.

[34] J. Sun, J. Yu, Q. Ma, F. Meng, X. Wei, Y. Sun, and N. Tsubaki, "Freezing copper as a noble metal–like catalyst for preliminary hydrogenation," *Sci. Adv.*, vol. 4, no. 12, pp. 1–15, Dec. 2018.
[35] A. Gargano and A. Timmermann, "Forecasting commodity price indexes using macroeconomic and financial predictors," *Int. J. Forecasting*, vol. 30, no. 3, pp. 825–843, Jul. 2014.
[36] K. Pearson, "Notes on regression and inheritance in the case of two parents," *Proc. Roy. Soc. London*, vol. 58, pp. 240–242, Jun. 1895.
[37] D. P. Kingma and J. Ba, "Adam: A method for stochastic optimization," in *Proc. 3rd Int. Conf. Learn. Represent.*, San Diego, CA, USA, May 2015, pp. 1–13.

FEI LI received the bachelor's degree in mechanical engineering from the Wuhan University of Technology, Hubei, China, in 1993, and the master's degree in mechanical engineering and the Ph.D. degree in computer science and applications from Zhejiang University, Hangzhou, China, in 1996 and 2004, respectively. In 2013, he joined the School of Computer and Computing Science, Hangzhou City University, as an Associate Professor. His research interests include the IoT, smart manufacturing, and computer software architecture.

HANLU ZHOU received the B.E. degree from the Shanghai University of Electric Power, in 2020, and the M.E. degree from Tongji University, in 2023. Her research interest includes intelligent manufacturing in the non-ferrous metal industry.

MIN LIU received the bachelor's degree in mechanical engineering from the China University of Geosciences, Wuhan, China, in 1993, and the master's degree in mechanical engineering and the Ph.D. degree in mechanical engineering and automation from Zhejiang University, Hangzhou, China, in 1996 and 1999, respectively. In 2001, he completed the Postdoctoral Research work from the Department of Computer Science, Shanghai JiaoTong University, China. From 2001 to 2004, he presided over the development of a large-scale supply chain software system for enterprises with Asia Bridge Software (China) Company. From 2007 to 2016, he visited the National Research Institute of Canada, the University of Western Ontario, Clemson University, the University of California, Los Angeles, the University of Florida, the University of Duisburg–Essen, Germany, and Coventry University, U.K. His research interests include fundamental theories, methods, and technologies for big data analysis and prediction, intelligent predictive maintenance, and intelligent manufacturing systems.

LEIMING DING received the B.E. degree from Huaibei Normal University, in 2020. He is currently pursuing the M.E. degree with the College of Computer Science (College of Software), Zhejiang University of Technology. His research interest includes few-shot learning.